# **High Temperature Insulation Materials for DC Cable** Insulation – Part III: Degradation and Surface Breakdown

# Chuanyang Li, Tohid Shahsavarian, Mohamadreza Arab Baferani, Ningzhen Wang, JoAnne Ronzello and Yang Cao

Electrical and Computer Engineering, University of Connecticut, 371 Fairfield Way, Storrs, CT 06269, USA

#### ABSTRACT

The first two parts in this series gave full analysis and discussion of five high temperature insulation materials, i.e. PTFE, FEP, ETFE, PEEK, and PI over aspects of space charge behavior, conduction property as well as partial discharge, respectively. In this part, the degradation and surface breakdown properties are investigated and the related mechanism is discussed. The results showed that due to stable formation of C-F structures, PTFE and FEP melted locally during arc erosion test, with no carbon element being precipitated. At 25 °C, PI showed the best surface anti-arc erosion property among ETFE, PEEK and PI. However, compared with other samples, the arc withstand property of PI can be much more influenced at higher temperature and in case of surface contamination. Compared with the results measured at 25 °C, the surface flashover voltage decreased for all samples when measured at 150 °C, which can be explained by the expansion of "analogous ineffective region". FEP has the highest surface flashover voltage at both 25 °C and 150 °C, which is due to higher surface roughness. The content of this paper provides a reference for aging characterization and evaluation of high temperature materials for DC cable and circuit board insulation.

Index Terms — DC cable, ETFE, PTFE, FEP, PI, PEEK, aging, surface flashover

# INTRODUCTION

**HIGH** temperature materials as insulation for DC cables and circuit boards are widely used in defense, aerospace, marine, precision instrument and other fields [1-5]. The reliable operation of high temperature insulation materials directly determines the stability of communication and power systems in extreme environments. In order to evaluate the reliability of different high temperature insulation materials in harsh operating environments, important aging factors must be studied in complex conditions. These factors mainly include space charge and surface charge transport behaviors [6-8], insulation breakdown and surface flashover trigger mechanism [9-12], insulation aging mechanisms and charge suppression methods [13–16], etc. However, uncertain factors in complex environments, such as the temperature variation due to the changing of engine output power, the gas pressure changes when aircraft reaches different altitudes, local contamination due to leakage of oil or environmental pollution, directly influence the insulation performance, leading to greatly increased complexity and difficulty for related fundamental and applied researches.

In part I, the space charge behaviors of five high temperature

insulation materials (PTFE, FEP, ETFE, PEEK, and PI) at

different temperatures were studied and the conduction of these material was measured and discussed [17]. Based on the results obtained from the first part, we further investigated the partial discharge property under DC voltage at different temperatures for the same materials, as is included in part II [18]. Accordingly, in this part, we focus on the degradation and surface flashover property of these five insulation materials. The surface arc resistance test and the surface flashover voltage test at different temperatures were performed and the mechanism for insulation degradation was investigated. Factors responsible for surface flashover voltage variations were studied and discussed. We hope the content of this series study can increase the attention and hence the understanding of high temperature insulation materials, and in addition, the results can help readers for better selection of PTFE, FEP, ETFE, PEEK, and PI based on specific insulation properties.

#### 2 EXPERIMENTAL

# 2.1 SAMPLE PREPARATION AND CHARACTERIZATION

The experimental samples are pure polymers of flat plaques with thicknesses of 320, 240, 240, 240 and 120 μm for PTFE, FEP, ETFE, PEEK and PI, respectively. The chemical composition, operating temperatures and applications of these samples are shown in Table 1.

Manuscript received on 11 June 2020, in final form 21 October 2020, accepted 26 October 2020. Corresponding author: Y. Cao.

 Table 1. Chemical composition analysis, operating temperatures and applications of samples.

Table 1. Chemical composition analysis, operating temperatures and applications of samples.				
Sample	Structural formula and FTIR spectrum	Corresponding structure	Operating temperature (OT) and Application	
PTFE	3500 3000 2500 2000 1500 1000 500 0  Wave number (cm <sup>-1</sup> )	Peaks at 1146 cm <sup>-1</sup> and 1200 cm <sup>-1</sup> correspond to stretching vibration of F-C-F bonds. Peaks at 509 cm <sup>-1</sup> , 554 cm <sup>-1</sup> , and 639 cm <sup>-1</sup> correspond to the bending vibration of F-C-F bonds.	OT: 200°C~260°C.  PTFE is widely used as high temperature material in atomic energy, national defense, aerospace, electronics, electrical, chemical, machinery, instruments, meters and other fields.	
FEP	$ \begin{array}{c ccccccccccccccccccccccccccccccccccc$	Peaks at 1146 cm <sup>-1</sup> and 1200 cm <sup>-1</sup> correspond to stretching vibration of F-C-F bonds. Peak at 982 cm <sup>-1</sup> corresponds to vibration of CF <sub>3</sub> groups. Peaks at 509 cm <sup>-1</sup> , 554 cm <sup>-1</sup> , and 639 cm <sup>-1</sup> correspond to bending vibration of F-C-F bonds.	OT: -80°C~205°C.  As a substitute for PTFE, FEP is widely used in transmission lines and electronic equipment under high temperature and high frequency, connection lines inside electronic computers, aerospace wires, special cables and motor wires.	
ETFE	The second secon	The vibrations corresponding to characteristic peaks of the $CF_2$ group in the range $1100{\sim}1400~\text{cm}^{-1}$ and the CH group in the range $900{\sim}1100~\text{cm}^{-1}$ .	OT: -80°C~220°C. ETFE is used as insulation in industrial wire and cable, nuclear reactor cable and vehicle wire, etc.	
PEEK	1217 1184 1187 1187 1184 11926 1113, 833 1645 1113, 833 166 1113, 833 166 1113, 833 167 1113, 833 1010 1010 500 0	Peak at 1645 cm <sup>-1</sup> corresponds to stretching vibration of C=O bonds. Peaks at 1593 cm <sup>-1</sup> and 1487 cm <sup>-1</sup> correspond to skeletal vibrations of the R-O-R aromatic ring structures. 1309 cm <sup>-1</sup> peak corresponds to plane vibrations of the R-OC-R aromatic ring structures. Peak at 1217 cm <sup>-1</sup> corresponds to asymmetric stretching vibration of R-O-R structures. 1184 cm <sup>-1</sup> , 1157 cm <sup>-1</sup> ,1113 cm <sup>-1</sup> , and 1010 cm <sup>-1</sup> peaks correspond to bending vibration of C-H in aromatic ring. 926 cm <sup>-1</sup> corresponds to symmetrical stretching vibration of R-OC-R structures. 833 cm <sup>-1</sup> and 766 cm <sup>-1</sup> peaks correspond to plane bending vibration of C-H in aromatic ring.	OT: -40°C~250°C. PEEK can replace traditional insulating materials such as metals and ceramics in many industry fields. PEEK is mainly used in aerospace, automotive industry, electronics and electrical, medical equipment and semiconductors, etc.	
PI	1710 1498 1115 1239 1080 1370 1775 1370 1370 1370 1370 1000 500 0	Peak at 1370 cm <sup>-1</sup> corresponds to stretching vibration of =C-N bonds. 1775 cm <sup>-1</sup> corresponds to asymmetric vibration of C=O structures. 1710 cm <sup>-1</sup> peak corresponds to symmetrical vibration of C=O structures. 1498 cm <sup>-1</sup> peak corresponds to skeletal vibration of aromatic ring. 1239 cm <sup>-1</sup> corresponds to symmetrical stretching vibration of C-O-C structures. Peak at 1115 cm <sup>-1</sup> corresponds to deformation vibration of C=O structures. 1080 cm <sup>-1</sup> peak corresponds to symmetrical stretching vibration of =C-H structures in aromatic ring.	OT: -200°C~300°C. PI is mainly used in electrical insulation of motors, magnetic conductors, aircraft and missile wiring, and flat flexible cables.	

Surface chemical compositions and structures of samples were tested using a Fourier Transform Infrared Spectrometer (NICOLET MAGNA 560). The surface morphology of experiment samples was examined by a field emission scanning electron microscope (JEOL JSM-6335F). Water contact angles were measured by using a hydrophobic test instrument (RAME HART MODEL 100 GONIOMETER).

#### 2.2 SURFACE ARC EROSION TEST

During the surface arc erosion test, two flat tungsten electrodes with tip pointing to each other were used as electrodes. The distance between the two electrodes was 8 mm. The samples under test were pressed under both electrodes and the arc frequency and power applied to the sample surface can be found in Table 2. The total time duration in each step is 60 seconds. The number of arcing was recorded until carbonized mark appeared on the sample surface and bridged both electrodes. materials.

Table 2. The arc frequency and power applied to the samples.

Step	Arc current	Arc duration	Arc frequency
1	10 mA	0.25 sec.	0.5Hz
2	10 mA	0.25 sec.	1Hz
3	10 mA	0.25 sec.	2Hz

#### 2.3 SURFACE FLASHOVER TEST

The test was performed at 25 and 150 °C, and fresh samples as received were cleaned using 75% anhydrous ethanol and placed in ambient environment for more than 24 hours before the test. To produce samples with contamination, the dimethyl silicone oil (CH<sub>3</sub>[Si(CH<sub>3</sub>)<sub>2</sub>]<sub>n</sub>Si(CH<sub>3</sub>)<sub>3</sub>) was painted on the sample surface as the contaminant. The electrode system was put in an oven to control the temperature and ten samples of each type were tested. It should be noted that as shown in Table 1, PTFE and FEP are formed by C-C bonds and C-F bonds which are more stable than C-H bonds. It is difficult for C-C bond scission to take place during arc erosion test and form carbonized marks on the sample surface. After the surface arc erosion test, the surfaces of PTFE and FEP showed a porous structure resulted from melting at high temperature during arcing. This phenomenon shows that these two materials do not have carbon precipitation caused by sample deterioration and thereby the surface arc erosion test was not used to evaluate these two. The DC surface flashover voltage test was carried out using the same electrode setup as in surface arc erosion test. The samples were placed on a ceramic holder and pressed closely under both electrodes with a distance of 7 mm between the electrode needles as shown in Figure 1. The electrode system was put in an oven to control the temperature and the voltage was increased with a ramping rate of 500 V/s. A current transformer was connected to the ground wire to detect the occurrence of surface flashover. Experimental samples were cleaned with 75% anhydrous ethanol and placed in ambient environment for more than 24 hours before the flashover test and each sample was tested two times.

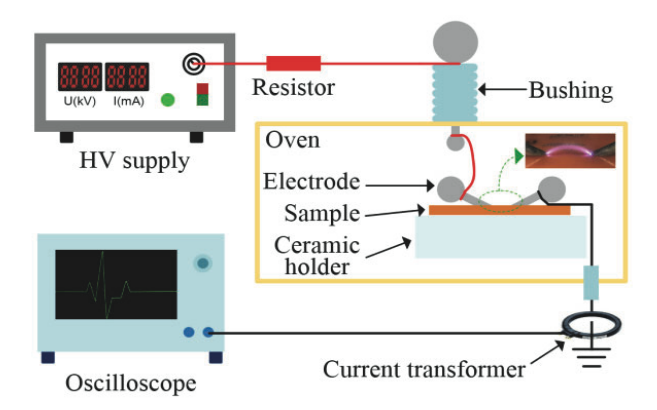
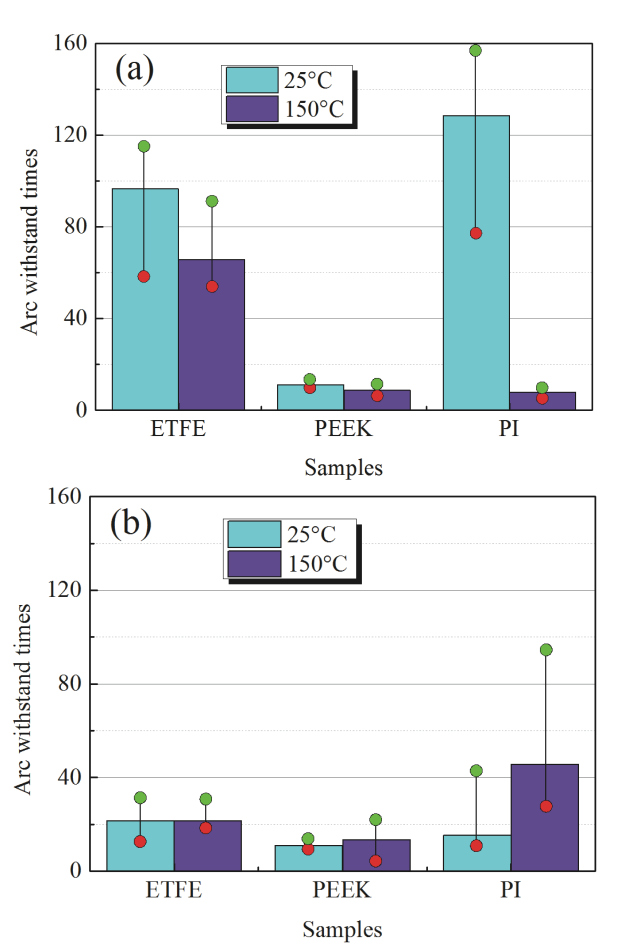


Figure 1. Setup of DC surface flashover test.

# 3 RESULTS

#### 3.1 SURFACE ARC EROSION TEST

Figure 2 shows surface arc withstand times for ETFE, PEEK and PI. It can be seen that among these three samples, PI has the highest arc withstand times of 130 at 25 °C. However, it can be inferred from its high dispersion that local surface micro defects and uneven distribution of materials during manufacturing may have a great impact on its anti-arc



**Figure 2.** Surface are withstand times for ETFE, PEEK and PI: (a) pure samples; (b) samples with surface oil contamination. The height of the histogram shows the average are withstand time. The green filled circles shows the highest are withstand time while the red filled circle shows the lowest are withstand time.

erosion property. It can also be verified that when the temperature was increased to 150 °C, its anti-arc erosion property was significantly reduced, with merely 10 rounds of arcs before carbonized trace was formed. ETFE showed a better performance than that of PEEK in arc erosion test at both 25 and 150 °C. Meanwhile, the anti-arc erosion property of PEEK is not sensitive to temperature, with no more than 20 rounds of arcing at both temperatures before carbon trace was formed across the surface. It is interesting to note that the surface carbonized marks were formed by the development of local carbonized spot, and once the localized carbonized point near electrodes appeared, the surface would soon develop into a carbonized trace.

When there was contaminant on the surface, the anti-arc erosion property of ETFE and PI at 25 °C was greatly reduced, dropping from arc withstand times of 89 and 130 to 20 and 18, respectively. However, the anti-arc aging property of PEEK was not affected, with an arc withstand times of 11 which was the same when measured using a pure sample. What surprised us is that at 150 °C, the anti-arc erosion property of samples with contamination increases, especially for ETFE and PI with arc withstand times of 14 and 47 which were higher than 11 and 17 measured at 25 °C. The anti-arc property of ETFE was not influenced at different temperatures, after the surface was contaminated.

#### 3.2 SURFACE MORPHOLOGY

Figure 3 shows the SEM results of the sample surface before and after arc erosion test. It can be observed that the surface of samples was smooth before arc erosion, except for FEP which contains nano-scaled unevenly distributed scratches. As it was mentioned in previous section, for PTFE and FEP during arc erosion, the materials melted during arcing and re-crystallized when the arc extinguished. After rearrangement of molecular chains, it can be seen that the scratches on the surface of FEP disappeared, which was replaced by a local smooth surface formed at the edge of holes. For ETFE, three features could be found on its surface after arc erosion test: local smooth regions being created by recrystallization, depressed regions which were due to degradation during arc erosion, and those perforated regions that can be formed due to local overheating during arcing. Compared to the above mentioned three samples, PEEK showed the most obvious surface degradation with severe carbonized areas after arcing, and highly roughened area near the edge of carbonized trace was formed with flaked carbon layers. For PI, the local carbonized zone was relatively concentrated, and the transition areas between the carbonized zone and the pure material were more obviously observed, in forms of cracks and localized small holes.

## 3.3 SURFACE FLASHOVER TEST

Figure 4 shows the DC surface flashover voltage of experiment samples. At 25 °C, the flashover voltage of samples was highly dispersed, ranging from 7.5 to 10 kV. Among all the samples, PTFE, FEP and ETFE had the highest surface flashover voltages, and the surface flashover voltage

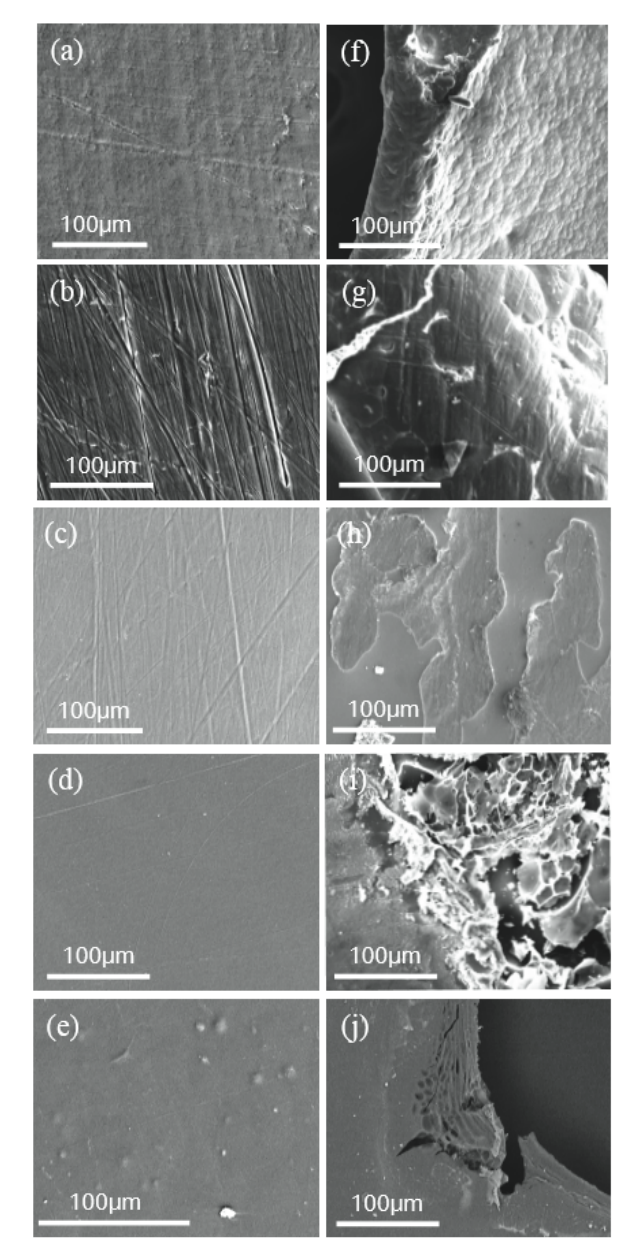


**Figure 3.** SEM results of samples before and after arc erosion test. (a)-(e) are SEM images of PTFE, FEP, ETFE, PEEK, and PI before surface arc erosion test, and (f)-(j) are SEM images of PTFE, FEP, ETFE, PEEK, and PI after surface arc erosion test.

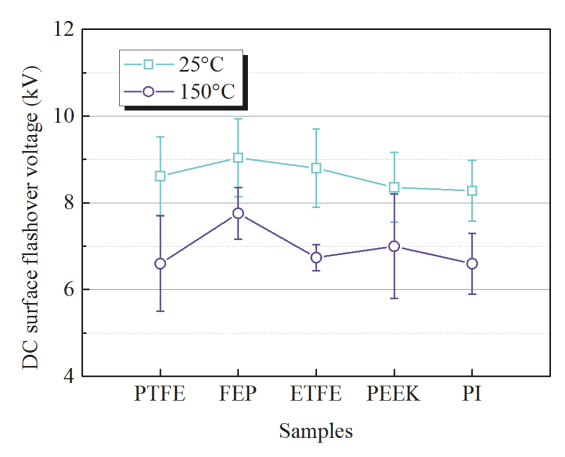


Figure 4. DC surface flashover voltage of experiment samples.

of PI was the lowest. Compared with the results measured at 25 °C, the surface flashover voltage at 150 °C showed decreasing trend within ranges from 5 to 8.5 kV. Still, FEP had the highest surface flashover voltage which reached 7.8 kV, while PTFE, ETFE, PEEK and PI had similar flashover voltages which were below 7kV. It is worth mentioning that the dispersion of surface flashover voltages for PTFE and PEEK were much higher than FEP, ETFE, and PI at higher temperature.

# 4 DISCUSSION

# **4.1 SURFACE ARC EROSION MECHANISM**

It has been illustrated that after arc erosion test, different samples showed different surface morphology. To further study the changes in material composition during surface arc erosion test, FTIR test was performed for experimental samples. Figure 5 shows the FTIR test results for PTFE, ETFE, and PI before and after surface arc erosion test. It can be found that the surface chemical composition of samples before and after arc erosion did not change. When there was no contamination on the surface, the C-H bonds in materials were broken and carbon elements were produced and attached on the insulation surface, forming the carbonized trace. Since the electrical conductivity of carbonized area is much higher compared with that of the pure insulation, when the carbonized area gradually grows along the insulation surface, current flows through the carbonized area more easily rather than in the form of arcs bending above the surface. At 150 °C,

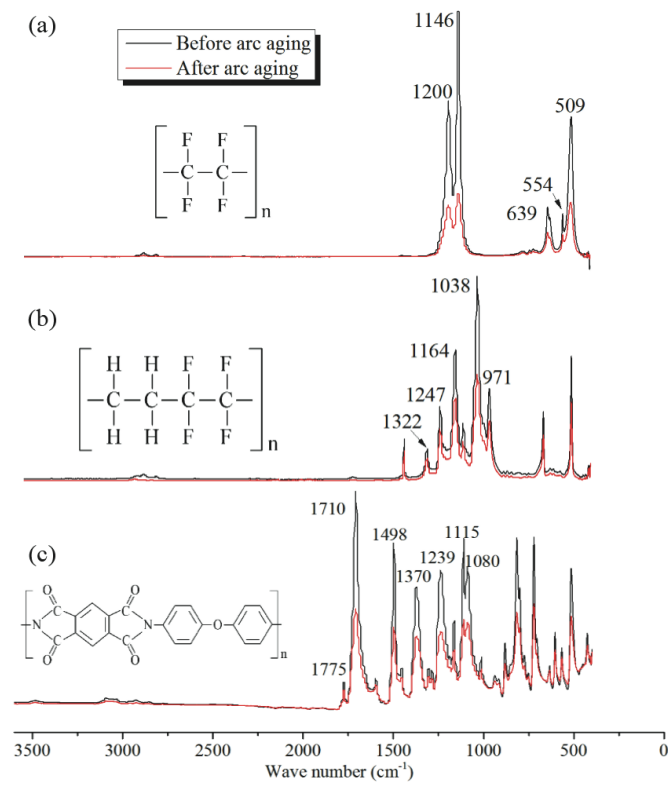


**Figure 5.** FTIR of samples before and after arc erosion test: (a) PTFE, (b) ETFE, and (c) PI. Note: For FEP and PEEK, the FTIR before and after arc erosion test were the same as that for the pure samples.

the entanglement between the molecular chain of the material becomes more separated, and the molecular chains movement is more intensified. In this case, the surface structure of the materials becomes much unstable, thereby reducing the arc withstand ability. This is the reason why surface arc withstand ability of samples at 150 °C is much lower than that at 25 °C.

PEEK has excellent high temperature operating characteristics. It has been found in Figure 2a that the effect of temperature change has very little effect on its anti-arc erosion property. However, the ultraviolet resistance of PEEK is much lower than other samples. It has been shown that UV treatment can effectively affect the chemical structure of PEEK surface and modify the wettability greatly [19]. The presence of strong ultraviolet rays in the arc can damage the chemical bonds of PEEK, resulting in a low anti-arc erosion property.

Unlike other materials, PI is a thermosetting material. It contains rigid groups of benzene rings and hydrogen bonds, which prevent it from deforming under higher temperature. However, when there is local pollution and defects, this rigid feature also causes the local heat which is difficult to dissipate, resulting in local high temperature. Once the local carbonized spot appears, it can develop into the carbonized traces across the surface.

When there is contaminant on the surface, the surface antiarc property is depended on the combined effect of the molecular chain movement and the surface contamination. Figure 6 shows the surface image of samples with and without surface contamination after arc erosion test. It can be found that when there is no contamination, penetrating carbonized marks appear on the surface for ETFE and PI. The arc erosion area shows a hole without evidence of carbonization. With contamination, the surface of samples after arc erosion test is covered by a white coating. The decomposition of dimethyl silicone oil in the presence of arcs generates CO<sub>2</sub>, SiO<sub>2</sub>, and H<sub>2</sub>O. This chemical reaction, together with the evaporation

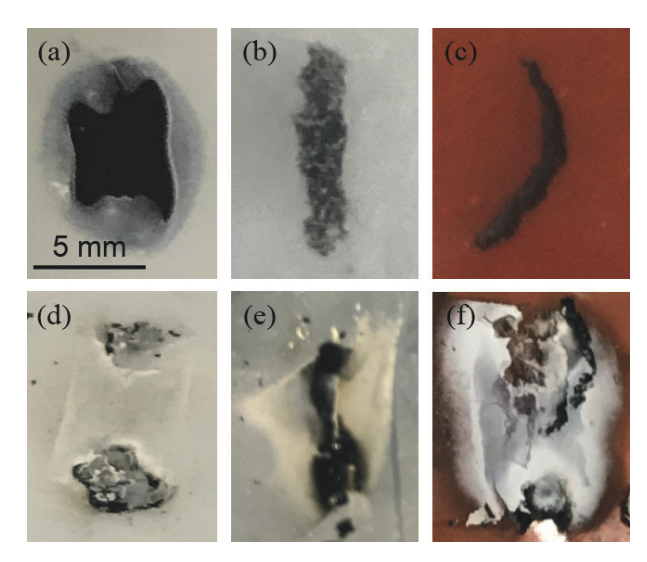


**Figure 6.** Images of surface erosion for samples with and without surface contamination: (a)-(c) are PTFE, ETFE, and PI without contamination; (d)-(f) are PTFE, ETFE, and PI with contamination. Note: For FEP and PEEK, the surface profile before and after arc erosion test were the similar as PTFE and PI.

of dimethyl silicone oil and H<sub>2</sub>O, takes away heat from the surface of the material, thereby improving the anti-arc erosion property. Meanwhile, as one of the decomposition by-products of dimethyl silicone oil, SiO2, which has good thermal conductivity than the polymer insulation, adheres to the insulation surface and promotes the dissipation of heat. At 150 °C, the dimethyl silicone oil is more uniformly distributed and a uniform SiO<sub>2</sub> coating can be formed between both electrodes. This explains why the contaminated sample has higher arc endurance capability at higher temperatures than that at 25 °C. However, for sample surface with contaminant at 25 °C, the anti-arc erosion capability is still lower than the surface without contaminant. We believe that the surface dimethyl silicone oil has poor fluidity at lower temperature and the surface oil film is unevenly distributed, resulting in a local overheating and aging, which makes it easier for degradation of the base insulation material. This hypothesis can be supported by the phenomenon that once local degradation occurs, the surface between electrodes is easier to develop into penetrating carbonized traces.

As an insulating dielectric material with heat resistance, corona resistance, corrosion resistance, moisture and dust resistance, dimethyl silicone oil is widely used in electrical machinery, electrical appliances, electronic instruments and other equipment. In addition, due to its excellent vibration absorption and temperature insensitivity, as liquid damper, the dimethyl silicone oil is also widely used in the landing gear of aircraft for vibration proof and damping. However, we would claim that in a real case some other contaminating oil might exist, which may result in different aging behavior due to its different properties.

# 4.2 FACTORS RESPONSIBLE FOR SURFACE FLASHOVER VOLTAGE VARIATIONS

The mechanism of surface flashover under DC is very complicated, which involves complicate physical processes including hetero-polar charge accumulation from gas ionization, homo-polar charge injection from electrode/ insulation interface, local nonlinear property of material, surface roughness, etc. It is shown from Figure 4 that the surface flashover voltage of different materials is slightly different. However, the surface flashover voltage of FEP at different temperatures is always the highest. We assume that this phenomenon is related to the surface roughness of FEP. As can be seen from Figure 2, there are evenly distributed scratches on the surface of FEP. It has been verified that the slightly increased rough surface structure has an effect on blocking the initial electron path of the electron collapse, thereby increasing the flashover voltage along the surface of the sample [20]. In addition, the surface water contact angle of samples was measured, which can be found in Figure 7. It can be seen that there is a positive correlation between the flashover voltage and the surface water contact angle at 25 °C. Among them, PTFE and FEP have the highest water contact angles of 105 and 106°, which are higher than 88 and 89° of ETFE and PEEK. This is consistent with the surface flashover voltage of experiment samples at 25 °C. A smaller surface

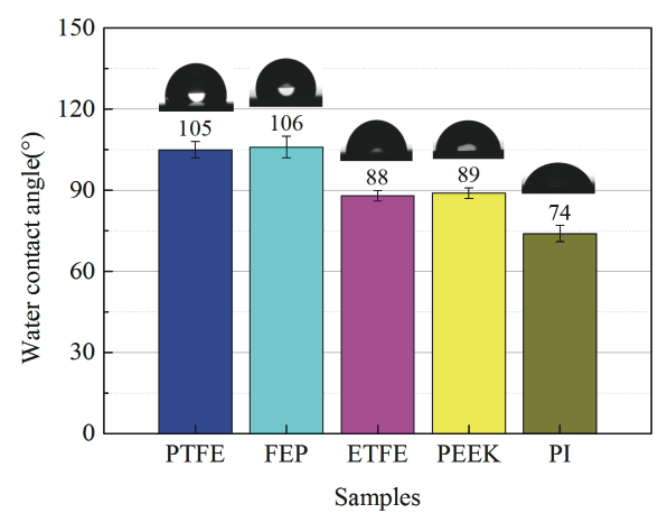


Figure 7. Surface water contact angle results.

water contact angle makes it easier for the surface to form local water films, which increases the surface conductivity and the tangential electric field component [21]. The increasing of the horizontal electric field decreases surface flashover voltage. This can explain why PI has the lowest surface flashover voltage at 25 °C. In addition, the increase of the horizontal electric field component correspondingly reduces the normal electric field component, thereby reducing the effect of the hetero-polar surface charge on the flashover voltage dispersion [11]. That is why PI has a smaller surface flashover voltage dispersion at 25 °C.

When the temperature is increased up to 150 °C, the effect of the water film on the surface is negligible. At this time, the effect of surface roughness, local conductivity and the injection of the homo-polarity charge on the surface flashover voltage become dominant. As shown in Figure 8, the conductivity of samples at 25 °C are lower than 1×10<sup>-14</sup> S/m [17]. It means that the effect of charge dissipation at normal temperature on surface flashover voltage is negligible. At 150 °C, we find that the conductivity of both ETFE and PI has been greatly improved with values of 1.59×10<sup>-11</sup> S/m and 4.49×10<sup>-12</sup> S/m, respectively. These values are nearly 4 orders of magnitude higher than the conductivity values measured at 25 °C. In this case, the temperature-dependent conductivity is regarded as the dominate parameter. As the conductivity increases, the locally accumulated charge dissipation rate increases, which greatly reduces the uncertainty of the surface flashover voltage [11]. This is why the dispersion of the PTFE and PEEK flashover voltages at 150 °C is much higher than those of the other three materials. In addition, the relatively high surface roughness of FEP is still the main reason responsible for the higher surface flashover voltage at higher temperature. In addition, the surface flashover voltages of samples decreased at high temperature. This is due to the increase of electric field strength near the ground electrode due to the injection of homo-polarity charges from the high voltage electrode. This can be explained by the theory of the expansion of "analogous ineffective region" as introduced in literature [22]. However, we have to admit that the nonlinear

property of surface conductivity of samples may influence the surface flashover voltage. As has already been noted in Part I, we had the conductivity of the samples measured at lower electric fields at 150 °C and no obvious increase in conductivity was found. However, it does not necessarily mean that the effect of the electric field is negligible since the electro-thermal effect on electrical conductivity is complicated. Further measurement will be performed to clarify the effect of electric field dependent surface conductivity.

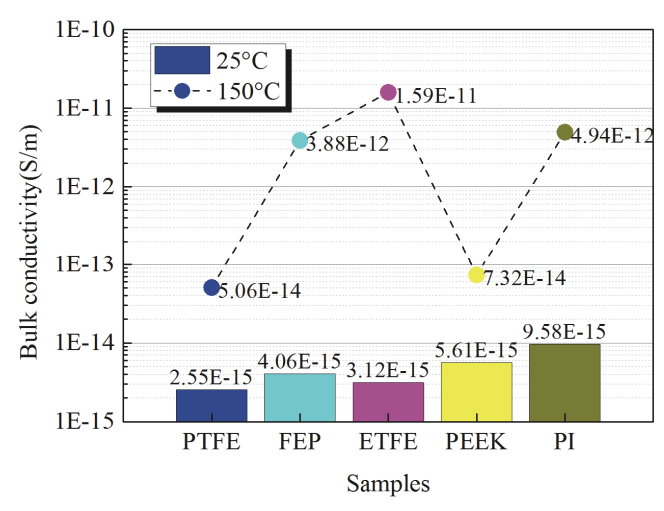


Figure 8. Bulk conductivity measured at 30 kV/mm in different temperatures [17].

## **5 CONCLUSIONS**

The stability of electrical properties of insulating materials in complex environments is essential for electrical equipment operating in harsh conditions. For example, being subjected to high temperature, humid, and radiation environments, the insulation of cables used in nuclear power plants may undergo hardening or cracking due to thermo-oxidative degradation and may become softening or swelling due to moisture intrusion under a moisture-related aging environment [23]. Meanwhile, the partial discharge inception voltage (PDIV) at 51kft could be 5 times lower compared with at sea level. This in turn poses higher challenges to the PD suppression and antiaging performance of cable and circuit board insulation materials operating in aircraft.

In part III, we studied the degradation and surface breakdown property of five high temperature materials, i.e. PTFE, FEP, ETFE, PEEK, and PI. The conclusions are drawn as follows:

- (1) Due to the composition of C-F and C-C structures, PTFE and FEP have better arc erosion property which show local melting instead of carbonized traces after arcing.
- (2) At 25 °C, PI shows best property among ETFE, PEEK and PI in surface arc erosion test. However, the arc withstand property of PI can be much influenced at higher temperature and in case of surface contamination.
- (3) The surface flashover voltage decreased for samples measured at 150 °C, which can be explained by the expansion of analogous ineffective region. FEP has the highest surface

flashover voltage at both 25 °C and 150 °C, which is due to the higher surface roughness.

(4) The increase in conductivity at 150 °C for FEP, ETFE and PI is responsible for the lower dispersion of surface flashover voltage, while at 25 °C, it is found that the surface water contact angle is positively correlated with the flashover voltage, which can be explained by the increase of the tangential electric field composite due to local surface water film.

This series of articles present the electrical properties of five commonly used high-temperature insulating materials, i.e. PTFE, FEP, ETFE, PEEK and PI. Firstly, we focused on the basic electrical properties and the space charge transport and conductivity characteristics at different temperatures were studied. Furthermore, we studied the partial discharge, flashover and aging behavior at different temperatures. Based on the results obtained in this series of articles, we found that PEEK shows both intense surface discharge and more space charge injection at the same condition compared with other four materials. The surface erosion test results of PEEK again prove a relatively poor behavior compared with other candidates. PTFE and PI have the lowest activation energy, from the viewpoint of which they may be better suitable for high temperature harsh environment applications. However, the arc withstanding property of PI decreases dramatically at high temperature and particularly in the case of surface contamination, which may limit the application of PI in harsh environment. The performance of ETFE is relatively good in both space charge test and particle discharge test. However, the higher temperature dependence of its conductivity can result in a homo-polar surface charge decay at higher temperature, which may result in a higher PD repetition rate.

However, the results we have obtained so far are still far from enough. The bulk breakdown and long-term aging mechanism of high-temperature insulation materials are not involved. In addition, studies in special operating conditions such as high humidity and air pressure variations, high field conditions and accelerated aging, as well as the research on surface charge behavior are merely mentioned. These directions will be the focus of our future research. In addition, the development of special insulation materials and improving the dielectric performance for special operating conditions will be a key point for our future work.

# **ACKNOWLEDGMENT**

The authors would like to thank NASA and United Technology Research Center, and the National Science Foundation (contract No. 1650544) for funding support. The authors would also like to thank Dr. Jim Guo of Techimp for helping with the partial discharge instrumentation and Dr. Mattewos Tefferi of G&W for suggestion with the PEA measurement.

# **REFERENCES**

[1] A. A. Sener and E. Demirhan, "The investigation of using magnesium hydroxide as a flame retardant in the cable insulation material by crosslinked polyethylene," Mater. Design, vol. 29, no.7, pp.1376–1379, 2008.

- [2] L. Li, et al., "Dielectric response of PTFE and ETFE wiring insulation to thermal exposure," IEEE Trans. Dielectr. Electr. Insul., vol. 17, no.4, pp.1234–1241, 2010.
- [3] S. Ochiai et al, "Thermally-stimulated current and dielectric loss measurement of polypropylene and Teflon-FEP films immersed in diarylethane," IEEE Trans. Dielectr. Electr. Insul., vol. 1, no. 3, pp. 487– 495, 1994.
- [4] N. Andreev et al, "Study of Kapton insulated superconducting coils manufactured for the LHC inner triplet model magnets at Fermilab," IEEE Trans. Dielectr. Electr. Insul., vol. 10, no. 1, pp. 119–122, 2000.
- [5] K. Barber and G. Alexander, "Insulation of electrical cables over the past 50 years," IEEE Electr. Insul. Mag., vol. 29, no. 3, pp. 27–32, 2013.
- [6] C. Y. Li et al, "The control mechanism of surface traps on surface charge behavior in alumina-filled epoxy composites," J. Phys. D: Appl. Phys., vol.49, p. 445304, 2016.
- [7] Z. P. Lei et al, "Mechanism of bulk charging behavior of ethylene propylene rubber subjected to surface charge accumulation," J. Appl. Phys., vol. 124, no. 24, p. 244103, 2018.
- [8] R. J. Men *et al*, "Effect of long-term fluorination on surface electrical performance of ethylene propylene rubber," High Voltage, vol. 4, no. 4, pp. 339–344, 2019.
- [9] C. Y. Li et al, "Novel HVDC spacers by adaptively controlling surface charges – part I: charge transport and control strategy," IEEE Trans. Dielectr. Electr. Insul., vol. 25, no. 4, pp. 1238–1247, 2018.
- [10] Y. Zhou, J. Hu, B. Dang, and J. L. He, "Effect of different nanoparticles on tuning electrical properties of polypropylene nanocomposites," IEEE Trans. Dielectr. Electr. Insul., vol. 24, no. 3, pp. 1380–1389, 2017.
- [11] C. Y. Li et al, "Field-dependent charging phenomenon of HVDC spacers based on dominant charge behaviors," Appl. Phys. Lett., vol. 114, no. 20, p. 202904, 2019.
- [12] C. Y. Li et al, "Charge cluster triggers unpredictable insulation surface flashover in pressurized SF<sub>6</sub>," J. Phys. D: Appl. Phys., doi.org/10.1088/1361-6463/abb38f, 2020.
- [13] T. Han et al, "Inhibition effect of graphene nanoplatelets on electrical degradation in silicone rubber," Polymers, vol. 11, no. 6, p. 968, 2019.
- [14] C. Y. Li et al, "Fluorine gas treatment improves surface degradation inhibiting property of alumina-filled epoxy composite," AIP Advances, vol. 6, p. 025017, 2016.
- [15] B. X. Du and Z. L. Li, "Hydrophobicity, surface charge and DC flashover characteristics of direct-fluorinated RTV silicone rubber," IEEE Trans. Dielectr. Electr. Insul., vol. 22, no. 2, pp. 934–940, 2015.
- [16] G. Teyssedre et al, "Charge recombination induced luminescence of chemically modified cross-linked polyethylene materials," IEEE Trans. Dielectr. Electr. Insul., vol. 16, pp. 232–240, 2009.
- [17] M. Arab Baferani et al, "High temperature insulation materials for DC cable insulation-Part I: Space charge and conduction," IEEE Trans. Dielectr. Electr. Insul., accepted.
- [18] T. Shahsavarian et al, "High temperature insulation materials for DC cable insulation Part II: Surface discharge," IEEE Trans. Dielectr. Electr. Insul., accepted.
- [19] H. Shi, J. Sinke, and R. Benedictus, "Surface modification of PEEK by UV irradiation for direct co-curing with carbon fibre reinforced epoxy prepregs," Int. J. Adhes. Adhes., vol. 73, pp. 51–57, 2017.
- [20] H. C. Miller, "Flashover of insulators in vacuum review of the phenomena and techniques to improve holdoff voltage," IEEE Trans. Dielectr. Electr. Insul., vol.28, no.4, pp. 512–527, 1993.
- [21] C. Y. Li, J. L. He, and J. Hu, "Surface morphology and electrical characteristics of direct fluorinated epoxy-resin/alumina composite," IEEE Trans. Dielectr. Electr. Insul., vol. 23, pp. 3071–3077, 2016.
- [22] C. Y. Li et al, "The neglected culprit of DC surface flashover-electron migration under temperature gradients," Sci. Rep., vol. 7, pp. 1–11, 2017.
- [23] Y. T. Hsu et al, "Correlation between mechanical and electrical properties for assessing the degradation of ethylene propylene rubber cables used in nuclear power plants," Polym. Degrad. Stabil., vol. 92, no. 7, pp. 1297–1303, 2007.



Chuanyang Li received his double B.S. degrees in electrical engineering and English in Taiyuan University of Technology. Then, he spent three years to obtain his M.S. degree from the Department of Electrical Engineering, Taiyuan University of Technology, from 2011 to 2014. He received his Ph.D degree in the Department of Electrical Engineering, Tsinghua University in 2018. He then worked as a

Postdoctoral Fellow at the Department of Electrical, Electronic and Information Engineering "Guglielmo Marconi" of the University of Bologna (Alma Mater Studiorum – Università Di Bologna), Italy from 2018 to 2019. From November 2019, he has been working in the Department of Electrical and Computer Engineering & Institute of Materials Science, University of Connecticut, as a Postdoctoral Fellow. His research interests include surface charge behavior and modification methods and PD properties of high temperature material in harsh conditions. He served as the Lead Guest Editor of the IEEE *Trans. Dielectr. Electr. Insul.* Special Issue on Advanced Dielectrics for Gas-Insulated Transmission Lines in 2018, Nanotechnology Focus Collection on Focus on Gas-Solid Interface Charging Physics in 2020, and the Guest Editor in High Voltage Special Issue on Interface Charging Phenomena for Dielectric Materials. He is an associate editor of IET High Voltage and CSEE JPES. He can be reached at lichuanyangsuper@163.com.



**Tohid Shahsavarian** was born in East Azerbaijan, Iran in 1989. He received the B.Sc. degree in electrical engineering from the University of Tabriz in 2011, and the M.Sc. degree from University of Science and Technology, Iran in 2013. Then, he worked in the Department of Transmission and Distribution at Monenco Iran Consulting Engineers Company. He is currently working toward the Ph.D. degree in electrical engineering at University of Connecticut. His research

interests include partial discharge analysis and risk assessment of AC and DC power cables, reliability analysis of HVDC grids, and geomagnetic disturbances.



Mohamadreza Arab Baferani received the BSc degree in electrical engineering from the Iran University of Science and Technology, Iran and MSc from University of Tehran, Iran. Currently, he is a PhD student in electrical engineering and research assistantship in University of Connecticut. His main research interests are high voltage engineering and HVDC cable systems.



Ningzhen Wang received her B.E. degree in 2013 from Huazhong University of Science and Technology, and Ph.D. degree in 2018 from Tsinghua University. She was a Ph.D. visiting student at Institut National des Sciences Appliquées de Lyon in 2017, and a postdoctoral fellow at Technische Universität Berlin from 2018 to 2019. Currently she is a postdoctoral researcher at the Electrical Insulation Research Center, University of Connecticut. Her research focuses on the

preparation, characterization and properties of metal foams and porous polymers, as well as device design of flexible wearable system.



JoAnne Ronzello is a research assistant at the Institute of Materials Science/Electrical Insulation Research Center at the University of Connecticut. JoAnne has spent more than 35 years working in the area of dielectrics including high voltage testing, failure analysis, dielectric spectroscopy, and novel experimental development. She holds undergraduate degrees in chemistry and electrical engineering.



Yang Cao graduated with B.S. and M.S. in physics from Tongji University in Shanghai, China, and received his PhD from the University of Connecticut in 2002, after which he served as a senior electrical engineer at GE Global Research Center until 2013. He is currently a full professor at the Electrical and Computer Engineering Department of the University of Connecticut. Dr. Cao is also the Director of the Electrical Insulation Research Center, Institute of Materials Science and the Site Director of the NSF

iUCRC Center on High Voltage/Temperature Materials & Structures. His research interests are in the physics of materials under extremely high field and the development of new dielectric materials, particularly the polymeric nanostructured materials, for energy efficient power conversion and renewables integrations, as well as for novel medical diagnostic imaging devices.